JACS
JOURNAL OF THE AMERICAN CHEMICAL SOCIETY
pubs.acs.org/JACS
Communication

Kinetically-Controlled Ni-Catalyzed Direct Carboxylation of Unactivated Secondary Alkyl Bromides without Chain Walking

Jacob Davies,[#] Julien R. Lyonnet,[#] Bjørn Carvalho, Basudev Sahoo, Craig S. Day, Francisco Juliá-Hernández, Yaya Duan, Álvaro Velasco-Rubio, Marc Obst, Per-Ola Norrby,[*] Kathrin H. Hopmann,[*] and Ruben Martin[*,#]

Cite This: J. Am. Chem. Soc. 2024, 146, 1753−1759
Read Online

ACCESS | Metrics & More | Article Recommendations | Supporting Information

ABSTRACT: Herein, we report the direct carboxylation of unactivated secondary alkyl bromides enabled by the merger of photoredox and nickel catalysis, a previously inaccessible endeavor in the carboxylation arena. Site-selectivity is dictated by a kinetically controlled insertion of CO_2 at the initial C(sp^3)−Br site by the rapid formation of Ni(I)−alkyl species, thus avoiding undesired β-hydride elimination and chain-walking processes. Preliminary mechanistic experiments reveal the subtleties of stereoelectronic effects for guiding the reactivity and site-selectivity.

Ni-catalyzed reductive carboxylation reactions with CO_2 have recently offered innovative replacements to existing protocols for preparing carboxylic acids,[1] which are privileged motifs in a myriad of biologically relevant molecules.[2] While these techniques have received considerable echo,[1] the utilization of secondary alkyl halides invariably results in carboxylation at distal C(sp^3)−H sites via chain walking irrespective of the position of the halide atom (Scheme 1, path a).[3] This is likely due to a particularly problematic CO_2 insertion at the initially generated C(sp^3)−Ni bond with site-selectivity of chain walking being dictated by a subtle interplay between electronic and steric effects. This observation has contributed to the perception that a catalytic direct carboxylation of unactivated secondary alkyl halides might represent a chimera, yet a worthwhile endeavor for chemical invention (path b).

Scheme 1. Carboxylation of Secondary Alkyl Halides

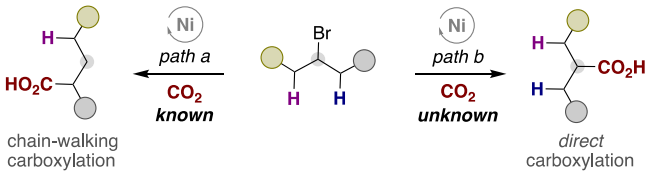

In our continuing interest in Ni-catalyzed carboxylations,[4,5] we wondered whether it would be possible to design a de novo catalytic carboxylation of unactivated secondary alkyl halides. Recent mechanistic studies have shown that CO_2 insertion predominantly occurs at well-defined Ni(I) centers.[6] We anticipated that accessing alkyl−Ni(I) species from unactivated secondary alkyl halides and low-valent NiL_n would be problematic with commonly employed heterogeneous metal reductants given (a) the low rates at which these entities promote single-electron transfer en route to alkyl−Ni(I)[7] and (b) the propensity of alkyl−Ni(II) species toward β-hydride elimination.[8] If successful, however, a study aimed at designing a retained Ni-catalyzed carboxylation of secondary alkyl halides would not only offer new opportunities in the carboxylation arena[1] but also a starting point for understanding the intricacies of Ni speciation in cross-couplings of sp^3 electrophiles.[9,10] Herein, we report the successful realization of this goal, which culminates in the development of a light-induced Ni-catalyzed retained carboxylation that operates under mild conditions and with excellent chemo- and site-selectivity profiles (Scheme 2, right).

We began our study by conducting the Ni-catalyzed carboxylation of **1a** with CO_2 (1 bar). Traces of **2a**, if any, were detected under previously reported Ni-catalyzed carboxylations of alkyl halides,[3,4] thus reinforcing the notion that a

Scheme 2. Site-Selectivity Guided by Ni Speciation

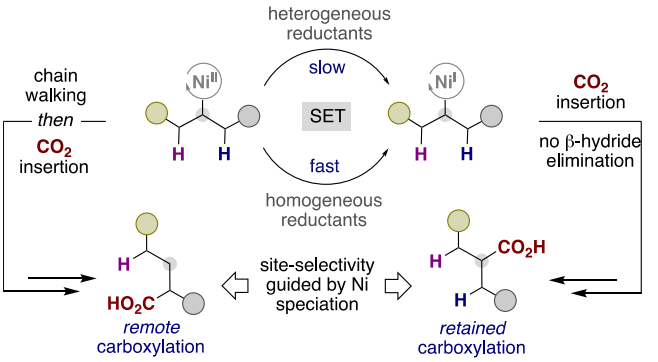

Received: October 10, 2023
Revised: December 19, 2023
Accepted: December 20, 2023
Published: January 9, 2024

Table 1. Scope of the Ni-Catalyzed Carboxylation of Secondary Alkyl Bromides[a]

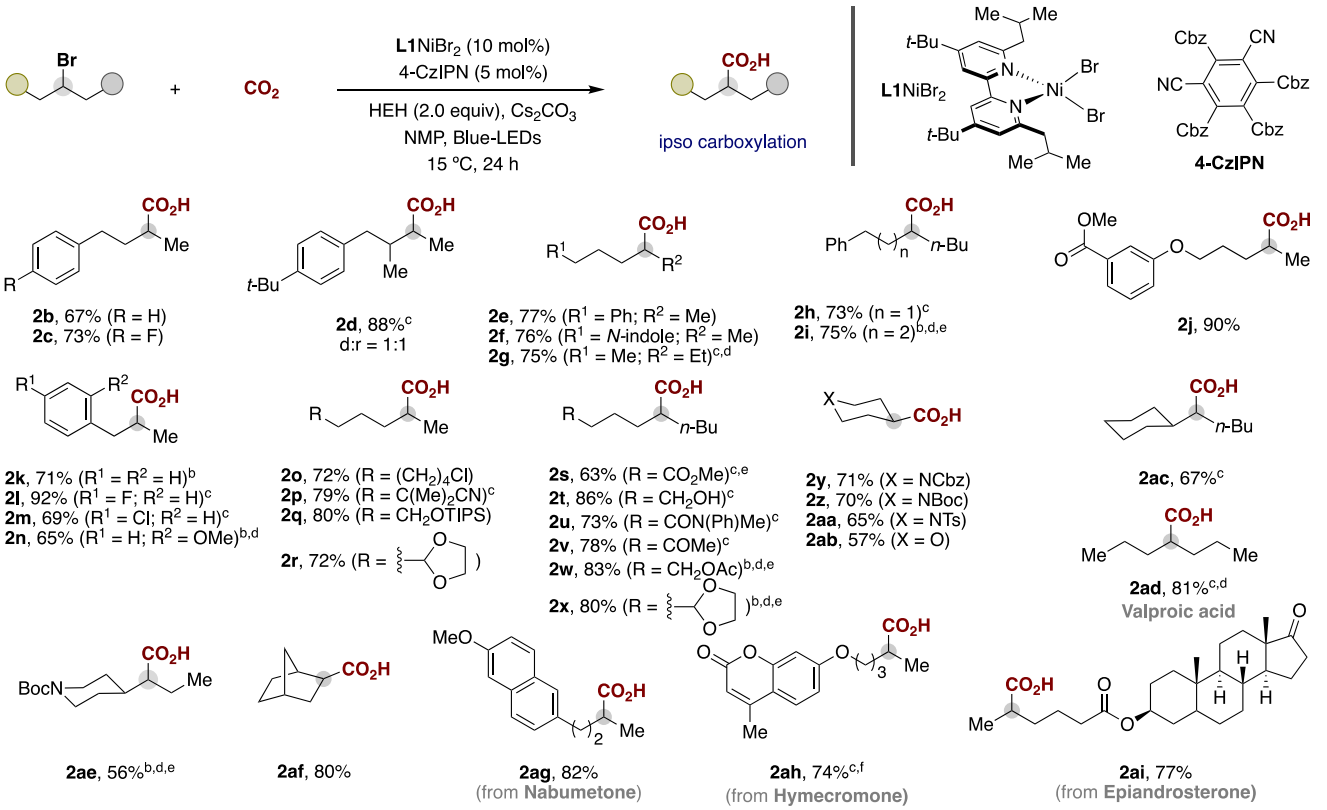

[a]Conditions: same as for Table 2. Isolated yields, average of at least two independent runs; branched/linear selectivities for **2a**–**2ai** rank from 8:1 to 99:1; see the Supporting Information for details. [b]4-CzIPN (10 mol %). [c]4-CzIPN (8 mol %). [d]Reaction ran at 10 °C. [e]Reaction conducted for 48 h. [f]HEH (3 equiv).

retained C(sp^3) carboxylation would be particularly problematic. After some experimentation,[11] a protocol utilizing **L1**, 4-CzIPN as photocatalyst, Cs_2CO_3, and Hantzch ester (HEH) in *N*-methyl-2-pyrrolidone (NMP) under blue LED irradiation at 15 °C provided the best results and afforded **2a** in 81% yield with excellent selectivity (99:1). Under these conditions, negligible CO_2 insertion at distal sp^3 C–H sites via chain walking was found in the crude reaction mixtures. As shown in entries 2–6, substituents at the 2,2′-bipyridine core exerted a profound influence in both reactivity and selectivity. Interestingly, low reactivities and selectivities were found at lower concentrations of 4-CzIPN, thus suggesting the importance for accessing alkyl–Ni(I) species prior to CO_2 insertion (entry 7).[12] In addition, bases and solvents other than Cs_2CO_3 and NMP resulted in low yields and selectivities (entries 8 and 9). Notably, the utilization of Mn or DMAP-OED[13] as reductants in lieu of 4-CzIPN/HEH resulted in little conversion, if any, to **2a** or lower branched selectivities,[11] thus confirming the significant influence exerted by photoredox-promoted electron transfer processes (entries 10 and 11). Control experiments revealed that all the reaction parameters were critical for success (entries 12 and 13), whereas no reaction took place with secondary alkyl iodides (**1a-I**), chlorides (**1a-Cl**), or tosylates (**1a-OTs**; see Scheme S7).

With the optimized conditions in hand, we set out to explore the generality of our retained carboxylation of unactivated secondary alkyl bromides. As shown in Table 1, our protocol turned out to be widely applicable. While low selectivities were found for secondary alkyl bromides possessing substituents other than methyl groups, this observation could be alleviated at higher concentrations of 4-CzIPN to obtain the targeted products with excellent branched selectivity (**2h**, **2s**–**x**). Notably, the inclusion of branched substituents or aromatic rings in the vicinity did not interfere with productive C(sp^3) carboxylation reaction (**2d**, **2k**–**n**).[4,10] The chemoselectivity of our method was further illustrated by the presence of esters (**2j**, **2s**, **2w**), amides (**2u**), unprotected alcohols (**2t**), heterocycles (**2f**, **2ah**) or nitriles (**2p**). Although one might argue that the presence of primary alkyl chlorides could lead to competitive carboxylation at the C(sp^3)–Cl site,[14] this was not the case, and **2o** was isolated in good yields. Note, however, that alkyl side chains possessing both a primary and secondary alkyl bromide led to complex mixtures of products.[11] In addition, no chain-walking carboxylation was observed with secondary alkyl halides decorated with esters or amides on the alkyl side chain.[4a,15] Along the same lines, no carboxylation adjacent to the nitrogen atom was observed when utilizing nitrogen- or oxygen-containing heterocycles (**2y**–**aa**, **2ab**, **2ae**).[16] As shown for **2ag**–**ai**, our method could also be utilized for accessing aliphatic carboxylic acids deriving from nabumetone (**2ag**), hymecromone (**2ah**), or epiandrosterone (**2ai**) in good yields and site-selectivities. In addition, valproic acid **2ad** was within reach in a high yield and site-selectivity.

Next, we turned our attention to studying the underpinnings of our carboxylation reaction (Scheme 3). To this end, we evaluated the reactivities of $(\mathbf{L1})_2$Ni(0) and **L1**Ni(I)Br. While the former was easily synthesized by simple exposure of **L1**$NiBr_2$ to Mg, comproportionation of Ni$(COD)_2$ and

https://doi.org/10.1021/jacs.3c11205
J. Am. Chem. Soc. 2024, 146, 1753–1759

Scheme 3. Preliminary Mechanistic Experiments

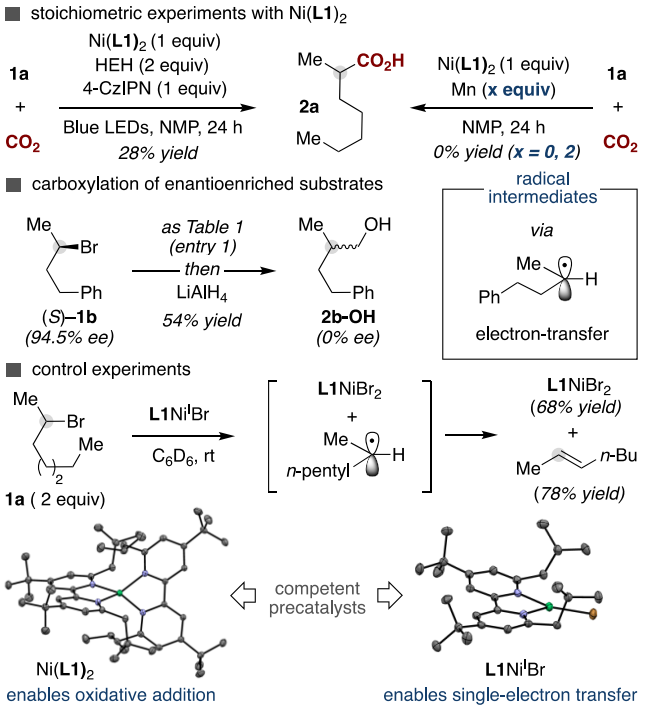

Scheme 4. Mechanistic Rationale and Isotope Labeling

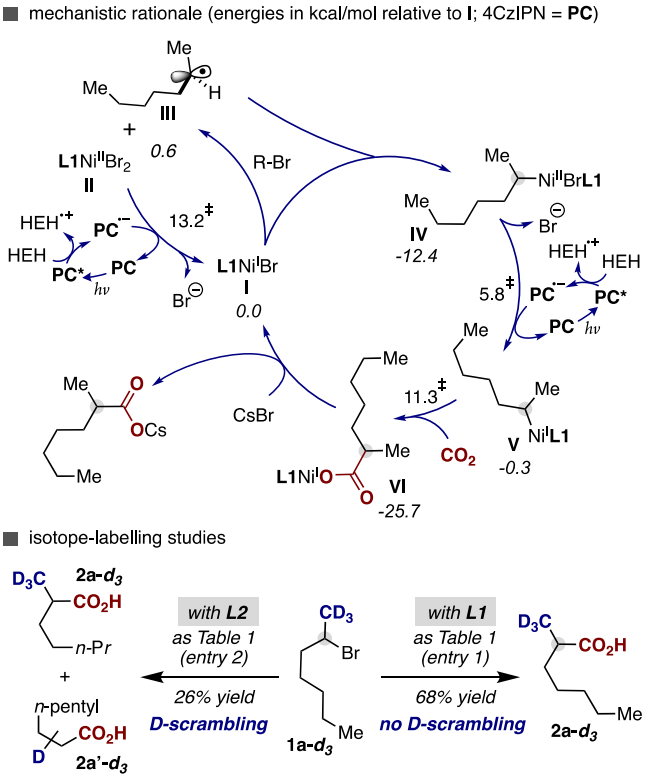

L1NiBr$_2$ was utilized to access the latter.[11] The structures of these compounds were unambiguously determined by X-ray diffraction (Scheme 3, bottom). Interestingly, the reaction of (**L1**)$_2$Ni(0) with **1a** under CO_2 (1 bar) did not give rise to **2a** (Scheme 3, top right). An otherwise identical reaction using **L1**Ni(I)Br led to *trans*-2-heptene as the major product. In contrast with an elegant report by Diao et al., this reaction also resulted in **L1**NiBr$_2$ instead of radical homocoupling.[17] Likely, this divergent reactivity originates from **L1**Ni(I)Br or **L1**Ni(II)Br$_2$ being able to readily intercept alkyl radicals prior to β-hydride elimination.[18] The means to generate discrete alkyl–Ni species was assessed by conducting an otherwise identical experiment with Mn or under a 4-CzIPN/HEH regime; while not even traces of **2a** were detected in the former, significant amounts of retained carboxylation were found in the latter, thus illustrating the non-negligible influence exerted by homogeneous reductants in both reactivity and selectivity (Scheme 3, top left). As anticipated for a mechanism consisting of radical intermediates, we observed a loss of stereochemical integrity when subjecting (S)-**1b** (94.5% ee) under a Ni/**L1** regime.

Aiming at understanding the intricacies of these processes at the molecular level, we turned our attention to DFT [PBE0-D3BJ,IEFPCM] calculations (Scheme 4). The reducing environment of our reaction conditions together with the tetrahedral center displayed for **L1**Ni(II)Br$_2$ and the preferred tetrahedral geometry of the four-coordinate Ni(I) species—imposed by the high-lying antibonding orbital dx^2-y^2—strongly suggests that the formation of Ni(I) may easily occur during the course of the catalytic carboxylation event.[19,20] Our theoretical calculations confirmed that single-electron transfer from the reduced photocatalyst to **L1**Ni(II)-Br$_2$ has a low barrier of 12.6 kcal/mol according to the Marcus equation.[21,22] Within the limitations from the solvent model employed, bromide dissociation from an in situ generated anionic Ni(I) complex was found to be downhill,[23] thus making the overall conversion from precatalyst **L1**Ni(II)Br$_2$ (**II**) to **L1**Ni(I)Br (**I**) exergonic by 0.4 kcal/mol.[24] Subsequently, the latter might react with alkyl bromide **1a** via bromide transfer, hence giving rise to **L1**Ni(II)Br$_2$ (**II**) and free radical **III** with a computed cost of only 0.6 kcal/mol (Scheme 4). Unfortunately, we did not locate a transition state for this process; at the DFT level, it seems this step might constitute a monotonous process without a potential energy barrier and, consequently, it might be diffusion-controlled. The loss of stereochemical information found for (*S*)–**1b** (Scheme 3, middle) is consistent with a pathway where radical **III** escapes the solvent cage. Interception of such species by a newly formed **I** was found to be strongly exergonic by 12.4 kcal/mol relative to **I** (Scheme 4).[25] The resulting **L1**Ni(II)-(alkyl)Br (**IV**) is particularly stable when compared with other Ni complexes within the catalytic cycle, thus suggesting that **IV** might represent the resting state. A barrier of 18.2 kcal/mol relative to **IV** was computed for single-electron transfer en route to **V** (Scheme 4). In analogy with recent literature data on alkyl–Ni(I) complexes,[6d] CO_2 insertion into **V** occurs with a low activation barrier (11.6 kcal/mol relative to **V**, Scheme 4 and Figure 1), thus giving a back-reaction barrier of 37.0 kcal/

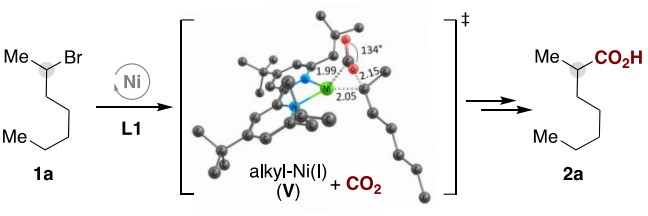

Figure 1. CO_2 insertion at alkyl–Ni(I)**L1**.

https://doi.org/10.1021/jacs.3c11205
J. Am. Chem. Soc. 2024, 146, 1753–1759

mol which makes the carboxylation step irreversible. Regeneration of the catalytically active **I** might involve transmetalation of **VI** to CsBr while forming a cesium carboxylate.[26]

Given the subtleties exerted by the ligand on the reaction outcome, we next focused our attention on understanding the erosion in selectivity observed with **L2** (Table 2, entry 2).

Table 2. Optimization of the Reaction Conditions[a]

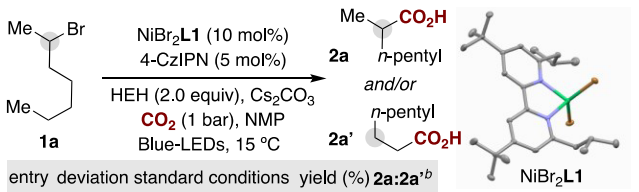

entry	deviation standard conditions	yield (%)	2a:2a'[b]
1	none	81(80)[c]	99:1
2	using $NiBr_2$**L2**	23	44:56
3	using $NiBr_2$**L3**	37	99:1
4	using $NiBr_2$**L4**	46	79:21
5	using $NiBr_2$**L5**	41	86:14
6	$NiBr_2$**L1** (5 mol%)	16	84:16
7	4-CzIPN (1 mol%)	29	88:12
8	K_2CO_3 instead of Cs_2CO_3	75	97:3
9	using DMA instead of NMP	52	84:16
10	using Mn instead of HEH	0	0
11	using DMAP-OED as reductant	9	44:56
12	no Cs_2CO_3	0	0
13	no $NiBr_2$**L1**, 4-CzIPN or light	0	0

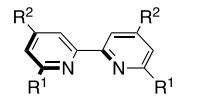

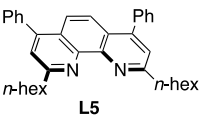

[a]Conditions: **1a** (0.25 mmol), $NiBr_2$**L1** (10 mol %), 4-CzIPN (5 mol %), HEH (0.5 mmol), Cs_2CO_3 (0.5 mmol), CO_2 (1 bar), and NMP (0.08 M) at 15 °C for 24 h under blue LED irradiation. [b]Other isomers were detected in negligible amounts; GC yields were obtained using anisole as an internal standard. [c]Isolated yield.

Initially, we conducted deuterium-labeling experiments with **1a-d$_3$** (Scheme 4, bottom). An erosion in deuterium content at C1 was expected for a mechanism consisting of a series of β-hydride elimination/migratory insertion, whereas preservation of the CD_3 fragment was anticipated for a rapid insertion of CO_2 at an in situ generated alkyl–Ni(I) species. As shown, **2a-d$_3$** was obtained as the only observable product with **L1** (Scheme 4, bottom right), whereas an otherwise identical experiment with **L2** resulted in deuterium scrambling over the alkyl chain (**2a′-d$_3$**, bottom left), which confirms the striking influence of the 2,2′-bipyridyl core on site-selectivity.[11]

Taking into consideration the proclivity of alkyl radical intermediates to undergo intramolecular hydrogen atom transfer (HAT) at proximal C(sp^3)–H bonds,[27] one might argue whether such a pathway could be responsible for the observable deuterium scrambling when promoting the carboxylation of **1a-d$_3$** under a Ni/**L2** regime (Scheme 4). Given that **III** diffuses away and re-enters the catalytic cycle at later stages to form **IV** and that the recombination of **III** with **I** might be diffusion-controlled (Scheme 4),[28] we turned our attention to DFT calculations for evaluating the viability of enabling HAT processes from the alkyl radical arising from **1a** (Scheme 5). While our results indicated that a 1,5- or 1,6-HAT from **III** could be within reach, the computed barriers are significantly larger than the expected barrier for recombination of **III** with Ni(I).[28] Indeed, neither **3** nor **4** were detected in the crude mixtures, thus arguing against the intermediacy of 1,5 or 1,6-HAT processes. While deuterium scrambling in the carboxylation of **1a-d$_3$** could also be rationalized by a formal

Scheme 5. Evaluation of Competitive HAT Processes[a]

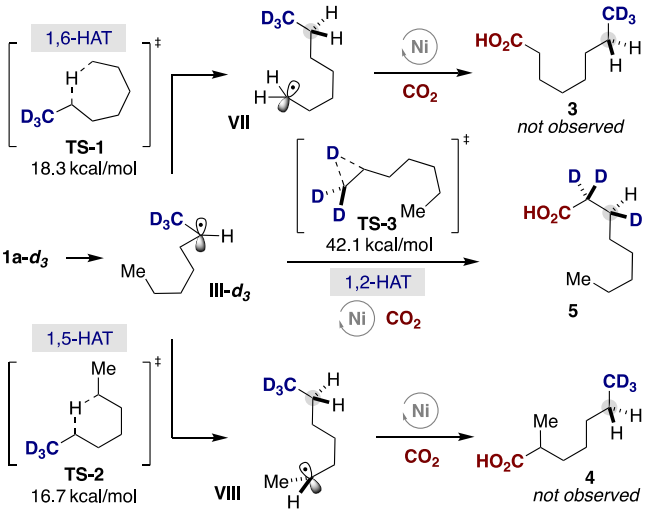

[a]The barriers were computed with **1a**.

1,2-HAT, the high barriers found for such a pathway (42.1 kcal/mol, Scheme 5) indicate otherwise. Although a base-mediated deprotonation from alkyl–Ni(III) species was also considered,[29] it is highly unlikely that such intermediates might be formed under strongly reducing conditions. Putting all these observations into consideration, the formation of **2a′-d$_3$** can be interpreted on the basis of a ligand-dependent β-hydride elimination event (for details, see the Supporting Information, Figure S8 and Table S5). With **IV** as the branching point, the reaction can evolve either via single-electron transfer en route to **V** or via β-hydride elimination arising from an initial loss of a bromide ion. Our data indirectly suggests that the steric bulk exerted by the substituents at the 6,6′-position in **L1** might disfavor the latter pathway, whereas a balanced situation between these pathways might occur with less-sterically encumbered **L2**.

In summary, we describe the successful implementation of a dual-photoredox, Ni-catalyzed direct carboxylation of unactivated secondary alkyl bromides, which is a previously inaccessible endeavor in the catalytic carboxylation arena. Experimental studies and theoretical calculations reveal an intriguing role exerted by the ligand backbone, which minimizes undesired β-hydride elimination events that might otherwise result in chain-walking scenarios while facilitating CO_2 insertion at alkyl–Ni(I) species. The method is characterized by its mild conditions, exquisite selectivity, and wide scope, including challenging substrate classes.

■ ASSOCIATED CONTENT

Supporting Information

The Supporting Information is available free of charge at https://pubs.acs.org/doi/10.1021/jacs.3c11205.

Computationally optimized structures (XYZ)
Experimental procedures and spectral and crystallographic data (PDF)

Accession Codes

CCDC 2250012–2250013 and 2250024 contain the supplementary crystallographic data for this paper. These data can be obtained free of charge via www.ccdc.cam.ac.uk/data_request/cif, or by emailing data_request@ccdc.cam.ac.uk, or by

https://doi.org/10.1021/jacs.3c11205
J. Am. Chem. Soc. 2024, 146, 1753–1759

contacting The Cambridge Crystallographic Data Centre, 12 Union Road, Cambridge CB2 1EZ, UK; fax: +44 1223 336033.

AUTHOR INFORMATION

Corresponding Authors

Per-Ola Norrby − *Data Science & Modelling, Pharmaceutical Sciences, R&D, AstraZeneca Gothenburg, SE-431 83 Mölndal, Sweden;* orcid.org/0000-0002-2419-0705; Email: Per-Ola.Norrby@astrazeneca.com

Kathrin H. Hopmann − *Department of Chemistry, UiT The Arctic University of Norway, N-9307 Tromsø, Norway;* orcid.org/0000-0003-2798-716X; Email: kathrin.hopmann@uit.no

Ruben Martin − *Institute of Chemical Research of Catalonia (ICIQ), The Barcelona Institute of Science and Technology, 43007 Tarragona, Spain; ICREA, 08010 Barcelona, Spain;* orcid.org/0000-0002-2543-0221; Email: rmartinromo@iciq.es

Authors

Jacob Davies − *Institute of Chemical Research of Catalonia (ICIQ), The Barcelona Institute of Science and Technology, 43007 Tarragona, Spain*

Julien R. Lyonnet − *Institute of Chemical Research of Catalonia (ICIQ), The Barcelona Institute of Science and Technology, 43007 Tarragona, Spain; Universitat Rovira i Virgili, Departament de Química Orgànica, 43007 Tarragona, Spain;* orcid.org/0000-0001-7466-5011

Bjørn Carvalho − *Department of Chemistry, UiT The Arctic University of Norway, N-9307 Tromsø, Norway*

Basudev Sahoo − *Institute of Chemical Research of Catalonia (ICIQ), The Barcelona Institute of Science and Technology, 43007 Tarragona, Spain;* orcid.org/0000-0002-9746-9555

Craig S. Day − *Institute of Chemical Research of Catalonia (ICIQ), The Barcelona Institute of Science and Technology, 43007 Tarragona, Spain; Universitat Rovira i Virgili, Departament de Química Orgànica, 43007 Tarragona, Spain;* orcid.org/0000-0002-6931-0280

Francisco Juliá-Hernández − *Institute of Chemical Research of Catalonia (ICIQ), The Barcelona Institute of Science and Technology, 43007 Tarragona, Spain;* orcid.org/0000-0001-5311-0957

Yaya Duan − *Institute of Chemical Research of Catalonia (ICIQ), The Barcelona Institute of Science and Technology, 43007 Tarragona, Spain*

Álvaro Velasco-Rubio − *Institute of Chemical Research of Catalonia (ICIQ), The Barcelona Institute of Science and Technology, 43007 Tarragona, Spain*

Marc Obst − *Department of Chemistry, UiT The Arctic University of Norway, N-9307 Tromsø, Norway*

Complete contact information is available at: https://pubs.acs.org/10.1021/jacs.3c11205

Author Contributions

#J. D. and J. R. L. contributed equally to the work.

Notes

The authors declare no competing financial interest.

ACKNOWLEDGMENTS

We thank ICIQ, FEDER/MCI PID2021-123801NB-I00, and European Research Council (ERC) under European Union's Horizon 2020 research and innovation program (grant agreement 883756) for financial support. K.H.H., M.O., and B.C. thank the support from the Research Council of Norway (No. 300769), NordForsk (Grant No. 85378) and the members of the Nordic Consortium for CO2 Conversion (NordCO2), and Sigma2 (Nos. nn9330k and nn4654k). J.R.L. and B.C. thank the European Union's Horizon 2020 research and innovation programme under the Marie Skłodowska-Curie grant agreement No 859910. C.S.D. thanks European Union's Horizon 2020 under the Marie Curie PREBIST grant agreement 754558. A.V.R. thanks MICINN and European Union (NextGenerationEU/PRTR) for a postdoctoral fellowship. We thank Prof. Feliu Maseras (ICIQ) for advice on computing SET barriers and Prof. Annette Bayer (UiT) and Prof. Luca Frediani (UiT) for fruitful discussions.

REFERENCES

(1) For selected reviews, see: (a) Tortajada, A.; Juliá-Hernández, F.; Börjesson, M.; Moragas, T.; Martin, R. Transition-Metal-Catalyzed Carboxylation Reactions with Carbon Dioxide. *Angew. Chem., Int. Ed.* **2018**, *57*, 15948. (b) Zhang, Z.; Ye, J.-H.; Ju, T.; Liao, L.-L.; Huang, H.; Gui, Y.-Y.; Zhou, W.-J.; Yu, D.-G. Visible-Light-Driven Catalytic Reductive Carboxylation with CO2. *ACS Catal.* **2020**, *10*, 10871. (c) Ye, J.-H.; Ju, T.; Huang, H.; Liao, L.-L.; Yu, D.-G. Radical Carboxylative Cyclizations and Carboxylations with CO2. *Acc. Chem. Res.* **2021**, *54*, 2518. (d) Davies, J.; Lyonnet, J. R.; Zimin, D. P.; Martin, R. The Road to Industrialization of Fine Chemical Carboxylation Reactions. *Chem.* **2021**, *7*, 2927. (e) Huang, W.; Lin, J.; Deng, F.; Zhong, H. Photocatalytic Carboxylation with CO2: A Review of Recent Studies. *Asian. J. Org. Chem.* **2022**, *11*, No. e202200220. (f) Tortajada, A.; Börjesson, M.; Martin, R. Nickel-Catalyzed Reductive Carboxylation and Amidation Reactions. *Acc. Chem. Res.* **2021**, *54*, 3941. (g) Chen, Y.-G.; Xu, X.-T.; Zhang, K.; Li, Y.-Q.; Zhang, L.-P.; Fang, P.; Mei, T.-S. Transition-Metal-Catalyzed Carboxylation of Organic Halides and Their Surrogates with Carbon Dioxide. *Synthesis* **2018**, *50*, 35−48.

(2) (a) Manallack, D. T.; Prankerd, R. J.; Nassta, G. C.; Ursu, O.; Oprea, T. I.; Chalmers, D. K. A Chemogenomic Analysis of Ionization Constants-Implications for Drug Discovery. *ChemMedChem.* **2013**, *8*, 242−255. (b) Oruç, T.; Küçük, S. E.; Sezer, D. Lipid Bilayer Permeation of Aliphatic Amine and Carboxylic Acid Drugs: Rates of Insertion, Translocation and Dissociation from MD Simulations. *Phys. Chem. Chem. Phys.* **2016**, *18*, 24511−24525. (c) Lou, Y.; Zhu, J. Carboxylic Acid Nonsteroidal Anti-Inflammatory Drugs (NSAIDs). In *Bioactive Carboxylic Compound Classes: Pharmaceuticals and Agrochemicals*; Lamberth, C., Dinges, J., Eds.; Wiley-VCH Verlag GmbH & Co. KGaA: Weinheim, Germany, 2016; pp 221−236.

(3) To the best of our knowledge, the catalytic carboxylation reaction of secondary alkyl(pseudo)halides from CO_2 has only been conducted on particularly activated benzyl/allyl systems or on C2-symmetric cyclic moieties where it is not possible to distinguish whether a chain-walking mechanism takes place or not. For selected examples of activated benzyl/allyl counterparts and cyclic systems, see: (a) Chen, B.-L.; Zhu, H.-W.; Xiao, Y.; Sun, Q.-L.; Wang, H.; Lu, J.-X. Asymmetric Electrocarboxylation of 1-Phenylethyl Chloride Catalyzed by Electrogenerated Chiral [CoI(Salen)]− Complex. *Electrochem. Commun.* **2014**, *42*, 55−59. (b) Moragas, T.; Cornella, J.; Martin, R. Ligand-Controlled Regiodivergent Ni-Catalyzed Reductive Carboxylation of Allyl Esters with CO2. *J. Am. Chem. Soc.* **2014**, *136*, 17702−17705. (c) Zhang, S.; Chen, W.-Q.; Yu, A.; He, L.-N. Palladium-Catalyzed Carboxylation of Benzyl Chlorides with Atmospheric Carbon Dioxide in Combination with Manganese/Magnesium Chloride. *ChemCatChem.* **2015**, *7*, 3972−3977. (d) Meng, Q.-Y.; Wang, S.; König, B. Carboxylation of Aromatic and Aliphatic Bromides and Triflates with CO2 by Dual Visible-Light-Nickel Catalysis. *Angew. Chem., Int. Ed.* **2017**, *56*, 13426−13430. (e) Sun, G.-Q.; Zhang, W.; Liao, L.-L.; Li, L.; Nie, Z.-H.; Wu, J.-G.;

Zhang, Z.; Yu, D.-G. Nickel-Catalyzed Electrochemical Carboxylation of Unactivated Aryl and Alkyl Halides with CO2. *Nat. Commun.* **2021**, *12*, 7086. (f) Wang, L.; Li, T.; Perveen, S.; Zhang, S.; Wang, X.; Ouyang, Y.; Li, P. Nickel-Catalyzed Enantioconvergent Carboxylation Enabled by a Chiral 2,2′-Bipyridine Ligand. *Angew. Chem., Int. Ed.* **2022**, *61* (51), No. e202213943. (g) Moragas, T.; Martin, R. Nickel-Catalyzed Reductive Carboxylation of Cyclopropyl Motifs with Carbon Dioxide. *Synthesis* **2016**, *48*, 2816.

(4) For examples, see: (a) Juliá-Hernández, F.; Moragas, T.; Cornella, J.; Martin, R. Remote Carboxylation of Halogenated Aliphatic Hydrocarbons with Carbon Dioxide. *Nature* **2017**, *545*, 84−88. (b) Sahoo, B.; Bellotti, P.; Juliá-Hernández, F.; Meng, Q.; Crespi, S.; König, B.; Martin, R. Site-Selective, Remote Sp3 C−H Carboxylation Enabled by the Merger of Photoredox and Nickel Catalysis. *Chem.—Eur. J.* **2019**, *25*, 9001−9005.

(5) For selected examples, see: (a) van Gemmeren, M.; Börjesson, M.; Tortajada, A.; Sun, S.-Z.; Okura, K.; Martin, R. Switchable Site-Selective Catalytic Carboxylation of Allylic Alcohols with CO2. *Angew. Chem., Int. Ed.* **2017**, *56*, 6558−6562. (b) Davies, J.; Janssen-Müller, D.; Zimin, D. P.; Day, C. S.; Yanagi, T.; Elfert, J.; Martin, R. Ni-Catalyzed Carboxylation of Aziridines En Route to β-Amino Acids. *J. Am. Chem. Soc.* **2021**, *143*, 4949−4954. (c) Börjesson, M.; Janssen-Müller, D.; Sahoo, B.; Duan, Y.; Wang, X.; Martin, R. Remote Sp2 C−H Carboxylation via Catalytic 1,4-Ni Migration with CO2. *J. Am. Chem. Soc.* **2020**, *142*, 16234−16239. (d) Tortajada, A.; Duan, Y.; Sahoo, B.; Cong, F.; Toupalas, G.; Sallustrau, A.; Loreau, O.; Audisio, D.; Martin, R. Catalytic Decarboxylation/Carboxylation Platform for Accessing Isotopically Labeled Carboxylic Acids. *ACS Catal.* **2019**, *9*, 5897−5901. (e) Tortajada, A.; Ninokata, R.; Martin, R. Ni-Catalyzed Site-Selective Dicarboxylation of 1,3-Dienes with CO2. *J. Am. Chem. Soc.* **2018**, *140*, 2050−205. (f) Liu, Y.; Cornella, J.; Martin, R. Ni-Catalyzed Carboxylation of Unactivated Primary Alkyl Bromides and Sulfonates with CO2. *J. Am. Chem. Soc.* **2014**, *136*, 11212−11215. and references therein.

(6) (a) Sayyed, F. B.; Tsuji, Y.; Sakaki, S. The Crucial Role of a Ni(i) Intermediate in Ni-Catalyzed Carboxylation of Aryl Chloride with CO2: A Theoretical Study. *Chem. Commun.* **2013**, *49*, 10715. (b) Sayyed, F. B.; Sakaki, S. The Crucial Roles of MgCl2 as a Non-Innocent Additive in the Ni-Catalyzed Carboxylation of Benzyl Halide with CO2. *Chem. Commun.* **2014**, *50*, 13026−13029. (c) Diccianni, J. B.; Hu, C. T.; Diao, T. Insertion of CO2Mediated by a (Xantphos)NiI−Alkyl Species. *Angew. Chem., Int. Ed.* **2019**, *58*, 13865−13868. (d) Somerville, R. J.; Odena, C.; Obst, M. F.; Hazari, N.; Hopmann, K. H.; Martin, R. Ni(I)−Alkyl Complexes Bearing Phenanthroline Ligands: Experimental Evidence for CO2 Insertion at Ni(I) Centers. *J. Am. Chem. Soc.* **2020**, *142*, 10936−10941. (e) Zhang, B.; Yang, S.; Li, D.; Hao, M.; Chen, B.-Z.; Li, Z. Insights into the Regioselective Hydrocarboxylation of Styrenes with CO2 Controlled by the Ligand of Nickel Catalysts. *ACS Sustainable Chem. Eng.* **2021**, *9*, 4091−4101.

(7) For selected reviews on Ni-catalyzed reductive couplings using metallic reductants, see: (a) Gu, J.; Wang, X.; Xue, W.; Gong, H. Nickel-Catalyzed Reductive Coupling of Alkyl Halides with Other Electrophiles: Concept and Mechanistic Considerations. *Org. Chem. Front.* **2015**, *2*, 1411. (b) Poremba, K. E.; Dibrell, S. E.; Reisman, S. E. Nickel-Catalyzed Enantioselective Reductive Cross-Coupling Reactions. *ACS Catal.* **2020**, *10*, 8237−8246. (c) Weix, J. D. Methods and Mechanisms for Cross-Electrophile Coupling of Csp2 Halides with Alkyl Electrophiles. *Acc. Chem. Res.* **2015**, *48*, 1767. (d) Moragas, T.; Correa, A.; Martin, R. Metal-Catalyzed Reductive Coupling Reactions of Organic Halides with Carbonyl-Type Compounds. *Chem. − Eur. J.* **2014**, *20*, 8242. (e) Knappke, C. E. I.; Grupe, S.; Gartner, D.; Corpet, M.; Gosmini, C.; Jacobi von Wangelin, A. Jacobi con Wangelin, A. Reductive Cross-Coupling Reactions between Two Electrophiles. *Chem. − Eur. J.* **2014**, *20*, 6828.

(8) For selected Ni-catalyzed C−C bond-forming reactions enabled by chain-walking reactions, see: (a) ref 4. (b) He, Y.; Cai, Y.; Zhu, S. Mild and Regioselective Benzylic C−H Functionalization: Ni-Catalyzed Reductive Arylation of Remote and Proximal Olefins. *J. Am. Chem. Soc.* **2017**, *139*, 1061−1064. (c) Lee, W.-C.; Wang, C.-H.; Lin, Y.-H.; Shih, W.-C.; Ong, T.-G. Tandem Isomerization and C−H Activation: Regioselective Hydroheteroarylation of Allylarenes. *Org. Lett.* **2013**, *15*, 5358−5361. (d) Bair, J. S.; Schramm, Y.; Sergeev, A. G.; Clot, E.; Eisenstein, O.; Hartwig, J. F. Linear-Selective Hydroarylation of Unactivated Terminal and Internal Olefins with Trifluoromethyl-Substituted Arenes. *J. Am. Chem. Soc.* **2014**, *136*, 13098−13101. (e) Peng, L.; Li, Y.; Li, Y.; Wang, W.; Pang, H.; Yin, G. Ligand-Controlled Nickel-Catalyzed Reductive Relay Cross-Coupling of Alkyl Bromides and Aryl Bromides. *ACS Catal.* **2018**, *8*, 310−313. (f) Wang, Z.; Yin, H.; Fu, G. C. Catalytic Enantioconvergent Coupling of Secondary and Tertiary Electrophiles with Olefins. *Nature* **2018**, *563*, 379−383. (g) Zhou, L.; Zhu, C.; Bi, P.; Feng, C. Ni-Catalyzed Migratory Fluoro-Alkenylation of Unactivated Alkyl Bromides with Gem -Difluoroalkenes. *Chem. Sci.* **2019**, *10*, 1144−1149. (h) Zhou, F.; Zhang, Y.; Xu, X.; Zhu, S. NiH-Catalyzed Remote Asymmetric Hydroalkylation of Alkenes with Racemic A-Bromo Amides. *Angew. Chem., Int. Ed.* **2019**, *58*, 1754−1758. (i) Zhang, Y.; Han, B.; Zhu, S. Rapid Access to Highly Functionalized Alkyl Boronates by NiH-Catalyzed Remote Hydroarylation of Boron-Containing Alkenes. *Angew. Chem., Int. Ed.* **2019**, *58*, 13860−13864. (j) Day, C. S.; Ton, S. J.; McGuire, R. T.; Foroutan-Nejad, C.; Martin, R. Reductive Elimination from Sterically Encumbered Ni-Polypyridine Complexes. *Organometallics* **2022**, *41*, 2662.

(9) For selected reviews on Ni-catalyzed cross-coupling of alkyl halides possessing β-hydrogens, see: (a) Netherton, M. R.; Fu, G. C. Nickel-Catalyzed Cross-Couplings of Unactivated Alkyl Halides and Pseudohalides with Organometallic Compounds. *Adv. Synth. Catal.* **2004**, *346*, 1525−1532. (b) Glorius, F. Asymmetric Cross-Coupling of Non-Activated Secondary Alkyl Halides. *Angew. Chem., Int. Ed.* **2008**, *47*, 8347−8349. (c) Hu, X. Nickel-Catalyzed Cross Coupling of Non-Activated Alkyl Halides: A Mechanistic Perspective. *Chem. Sci.* **2011**, *2*, 1867. (d) Shi, R.; Zhang, Z.; Hu, X. Nickamine and Analogous Nickel Pincer Catalysts for Cross-Coupling of Alkyl Halides and Hydrosilylation of Alkenes. *Acc. Chem. Res.* **2019**, *52*, 1471−1483.

(10) For selected reviews on chain-walking reactions, see: (a) Kochi, T.; Kanno, S.; Kakiuchi, F. Nondissociative Chain Walking as a Strategy in Catalytic Organic Synthesis. *Tetrahedron Lett.* **2019**, *60*, 150938. (b) Janssen-Müller, D.; Sahoo, B.; Sun, S.; Martin, R. Tackling Remote Sp3 C−H Functionalization via Ni-Catalyzed "Chain-walking" Reactions. *Isr. J. Chem.* **2020**, *60*, 195−206. (c) Fiorito, D.; Scaringi, S.; Mazet, C. Transition Metal-Catalyzed Alkene Isomerization as an Enabling Technology in Tandem, Sequential and Domino Processes. *Chem. Soc. Rev.* **2021**, *50*, 1391−1406. (d) Scaringi, S.; Mazet, C. Transition Metal-Catalyzed (Remote) Deconjugative Isomerization of α,β-Unsaturated Carbonyls. *Tetrahedron Lett.* **2022**, *96*, 153756. (e) Wang, Y.; He, Y.; Zhu, S. NiH-Catalyzed Functionalization of Remote and Proximal Olefins: New Reactions and Innovative Strategies. *Acc. Chem. Res.* **2022**, *55*, 3519−3536. (f) Sommer, H.; Juliá-Hernández, F.; Martin, R.; Marek, I. Walking Metals for Remote Functionalization. *ACS Cent. Sci.* **2018**, *4*, 153.

(11) See the Supporting Information for details.

(12) We observed a linear relationship of site-selectivity with the concentration of 4-CzIPN, thus showcasing the reliance on faster single-electron transfer kinetics. See the Supporting Information for details.

(13) Charboneau, D. J.; Brudvig, G. W.; Hazari, N.; Lant, H. M. C.; Saydjari, A. K. Development of an Improved System for the Carboxylation of Aryl Halides through Mechanistic Studies. *ACS Catal.* **2019**, *9*, 3228−3241.

(14) Börjesson, M.; Moragas, T.; Martin, R. Ni-Catalyzed Carboxylation of Unactivated Alkyl Chlorides with CO2. *J. Am. Chem. Soc.* **2016**, *138*, 7504−7507.

(15) For Ni-catalyzed chain-walking reactions controlled by pending ester or amide groups, see: (a) Chen, X.; Rao, W.; Yang, T.; Koh, M. J. Alkyl Halides as Both Hydride and Alkyl Sources in Catalytic Regioselective Reductive Olefin Hydroalkylation. *Nat. Commun.*

https://doi.org/10.1021/jacs.3c11205
J. Am. Chem. Soc. 2024, 146, 1753−1759

2020, *11*, 5857. (b) Lee, C.; Seo, H.; Jeon, J.; Hong, S. γ-Selective C(Sp3)−H Amination via Controlled Migratory Hydroamination. *Nat. Commun.* **2021**, *12*, 5657. (c) Wang, X.-X.; Xu, Y.-T.; Zhang, Z.-L.; Lu, X.; Fu, Y. NiH-Catalysed Proximal-Selective Hydroalkylation of Unactivated Alkenes and the Ligand Effects on Regioselectivity. *Nat. Commun.* **2022**, *13*, 1890. (d) Zheng, S.; Wang, W.; Yuan, W. Remote and Proximal Hydroaminoalkylation of Alkenes Enabled by Photoredox/Nickel Dual Catalysis. *J. Am. Chem. Soc.* **2022**, *144*, 17776−17782. (e) Rodrigalvarez, J.; Wang, H.; Martin, R. Native Amides as Enabling Vehicles for Forging Sp3−Sp3 Architectures via Interrupted Deaminative Ni-Catalyzed Chain-Walking. *J. Am. Chem. Soc.* **2023**, *145*, 3869−3874.

(16) (a) Zhao, L.; Zhu, Y.; Liu, M.; Xie, L.; Liang, J.; Shi, H.; Meng, X.; Chen, Z.; Han, J.; Wang, C. Ligand-Controlled NiH-Catalyzed Regiodivergent Chain-Walking Hydroalkylation of Alkenes. *Angew. Chem. Int. Ed* **2022**, *61*, No. e202204716. (b) Yang, P.; Shu, W. Orthogonal Access to A-/B-Branched/Linear Aliphatic Amines by Catalyst-Tuned Regiodivergent Hydroalkylations. *Angew. Chem. Int. Ed* **2022**, *61*, No. e202208018. (c) Wang, J.; Liu, D.; Chang, Z.; Li, Z.; Fu, Y.; Lu, X. Nickel-Catalyzed Switchable Site-Selective Alkene Hydroalkylation by Temperature Regulation. *Angew. Chem. Int. Ed* **2022**, *61*, No. e202205537.

(17) Lin, Q.; Diao, T. Mechanism of Ni-Catalyzed Reductive 1,2-Dicarbofunctionalization of Alkenes. *J. Am. Chem. Soc.* **2019**, *141*, 17937−17948.

(18) Lin, Q.; Spielvogel, E. H.; Diao, T. Carbon-Centered Radical Capture at Nickel(II) Complexes: Spectroscopic Evidence, Rates, and Selectivity. *Chem.* **2023**, *9*, 1295−1308.

(19) While single-electron transfer reduction of four-coordinate Ni(II) centers might lead to trigonal planar Ni(I) structures, it is fair to assume that the presence of polar aprotic solvents, such as NMP, might occupy a vacant coordination site, thereby resulting in a four-coordinate, tetrahedral geometry for Ni(I).

(20) The inclusion of substituents adjacent to the nitrogen motif in the 2,2′-bipyridine and 1,10-phenanthroline series has been found to impose tetrahedral or heavily distorted square planar geometries in a number of Ni(II) complexes employed for reductive coupling events. For selected references, see: (a) Börjesson, M.; Moragas, T.; Martin, R. Ni-catalyzed carboxylation of unactivated alkyl chlorides with CO2. *J. Am. Chem. Soc.* **2016**, *138*, 7504. (b) Serrano, E.; Martin, R. Nickel-catalyzed reductive amidation of unactivated alkyl bromides. *Angew. Chem., Int. Ed.* **2016**, *55*, 11207. (c) Somerville, R. J.; Odena, C.; Obst, M. F.; Hazari, N.; Hopmann, K. H.; Martin, R. Ni(I)-alkyl complexes bearing phenanthroline ligands: experimental evidences for CO2 insertion at Ni(I) centers. *J. Am. Chem. Soc.* **2020**, *142*, 10936. (d) Day, C. S.; Ton, S. J.; McGuire, R. T.; Foroutan-Nejad, C.; Martin, R. Reductive elimination from sterically encumbered Ni-polypyridine complexes. *Organometallics* **2022**, *41*, 2662. (e) Day, C. S.; Rentería-Gomez, A.; Ton, S. J.; Gogoi, A. R.; Gutierrez, O.; Martin, R. Elucidating electron-transfer events in polypyridine nickel complexes for reductive coupling reactions. *Nat. Catal.* **2023**, *2023*, 244. (f) Dietrich-Buchecker, C. O.; Guilhem, J.; Kern, J.-M.; Pascard, C.; Sauvage, J.-P. Molecular structures of a monovalent and a divalent nickel catenate: competition between metal orbital requirements and geometrical constraints imposed by the ligand. *Inorg. Chem.* **1994**, *33*, 3498.

(21) See the Supporting Information, Table S3.

(22) For details on the single-electron transfer process, see the Supporting Information, Figure S5.

(23) See the Supporting Information, Table S4.

(24) See the Supporting Information, Figure S12.

(25) In sharp contrast, interception of radical **III** by **II** en route to possible Ni(III) species was found to be endergonic by 10 kcal/mol relative to **I**. See the Supporting Information, Figure S13.

(26) CsBr aggregates might be expected to form under the reaction conditions because of the presence of Cs cations and Br anions.

(27) For selected reviews, see: (a) Capaldo, L.; Ravelli, D.; Fagnoni, M. Direct photocatalyzed hydrogen atom transfer (HAT) for aliphatic C−H bonds elaboration. *Chem. Rev.* **2022**, *122*, 1875−1924. (b) Cao, H.; Tang, X.; Tang, H.; Yuan, Y.; Wu, J. Photoinduced intermolecular hydrogen atom transfer reactions in organic synthesis. *Chem. Catal.* **2021**, *1*, 523−598. (c) Stateman, L.; Nakafuku, K.; Nagib, D. Remote C−H functionalization via selective hydrogen atom transfer. *Synthesis* **2018**, *50*, 1569−1586.

(28) While recombination is diffusion-controlled, it has a small apparent barrier (∼4.5 kcal/mol) at the standard state [1 M of Ni(I) species **I**], which increases by ∼1.4 kcal/mol for each order of magnitude lower concentration. For the HAT process to be competitive, the concentration of Ni(I) would, therefore, need to be lower than ∼10−8 M, which is a rather unlikely scenario; see: McMullin, C. L.; Jover, J.; Harvey, J. N.; Fey, N. Accurate Modelling of Pd(0) + PhX Oxidative Addition Kinetics. *Dalton Trans* **2010**, *39*, 10833−10836.

(29) See the Supporting Information, Figure S9.

https://doi.org/10.1021/jacs.3c11205
J. Am. Chem. Soc. 2024, 146, 1753−1759